R_{AA} and v_n : relativistic transport approach for charm and bottom toward a more solid phenomenological determination of $D_s(T)$

S. Plumari

Dipartimento di Fisica e Astronomia 'E. Majorana', Università degli Studi di Catania

INFN-LNS

Thanks to:
M.L. Sambataro, V. Minissale, G. Parisi, Y. Sun, V. Greco

ICHEP 2024 | PRAGUE
17–24 Jul 2024
Prague

Heavy quarks in uRHIC

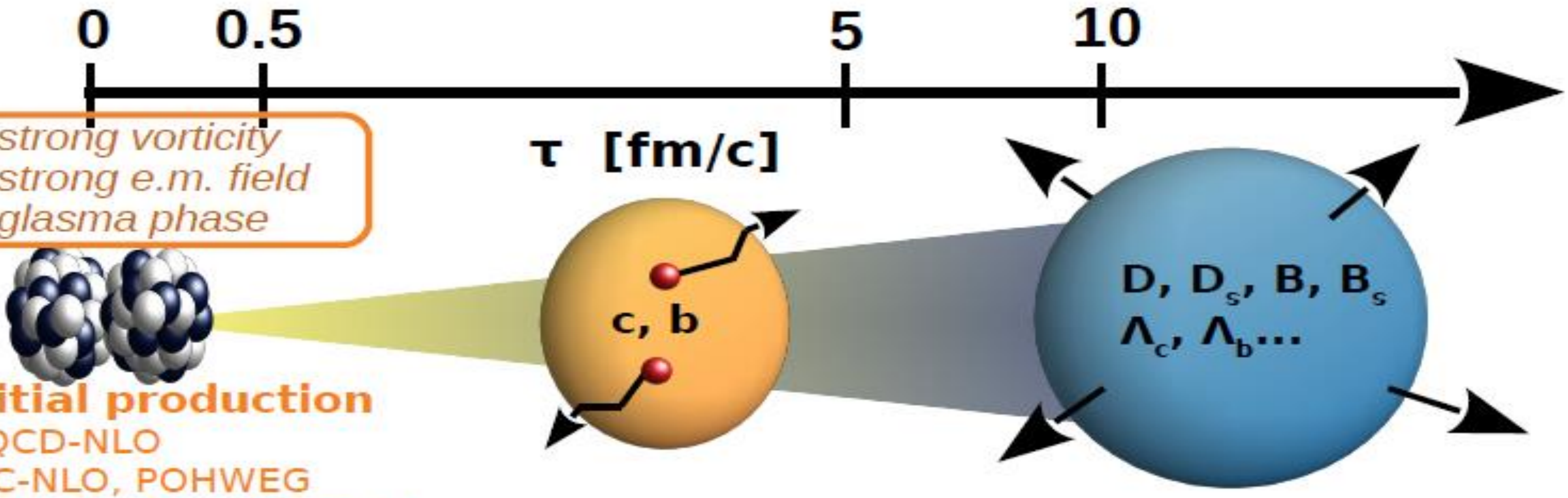

- *strong vorticity*
- *strong e.m. field*
- *glasma phase*

Initial production
- pQCD-NLO
- MC-NLO, POHWEG
- CNM effect[pp,pA exp.]

$$\sigma_{pp\to c\bar{c}} = \int_0^1 dx_1 dx_2 \sum_{i,j} f_i(x_1, Q^2) f_j(x_2, Q^2) \sigma_{ij\to c\bar{c}}(x_1, x_2, Q^2),$$

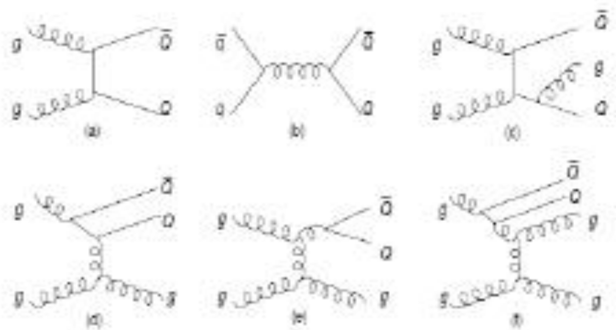

Dynamics in QGP
- Transport approaches: Boltzmann/Fokker-Planck
- Themalization
- Transp. Coeff. of QCD matter $D_s(T)$
- Jet Quenching

Hadronization
- SHM/coalescence and/or fragm. D, D_s, B, B_s, Λ_c, Λ_b, Ξ_c, Ω_c...
- Λ_c/D in pp,pA,AA
- R_{AA}, collective flow harmonics

Reviews:
X.Dong, V. Greco Prog. Part. Nucl. Phys. 104 (2019),
A.Andronic EPJ C76 (2016), 3) R.Rapp, F.Prino J.Phys. G43 (2016)

Relativistic Boltzmann eq. at finite η/s

Bulk evolution

$$p^{\mu}\partial_{\mu}f_q(x,p) + m(x)\partial_{\mu}^{x}m(x)\partial_{p}^{\mu}f_q(x,p) = C[f_q,f_g]$$

$$p^{\mu}\partial_{\mu}f_g(x,p) + m(x)\partial_{\mu}^{x}m(x)\partial_{p}^{\mu}f_g(x,p) = C[f_q,f_g]$$

free-streaming | field interaction $\varepsilon-3p\neq0$ | collision term gauged to some $\eta/s\neq0$

Equivalent to viscous hydro $\eta/s\approx0.1$

S. Plumari et al.,J.Phys.Conf.Ser. 981 012017 (2018).

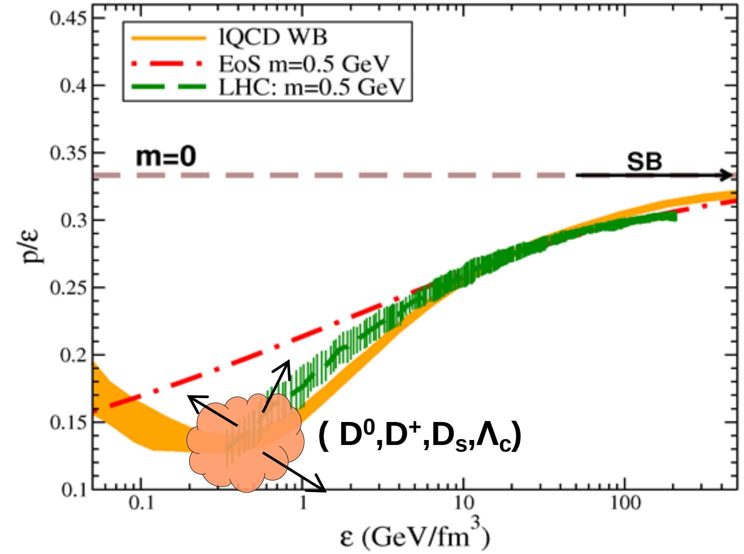

HQ evolution

$$p^{\mu}\partial_{\mu}f_Q(x,p) = \mathcal{C}[f_q,f_g,f_Q](x,p)$$

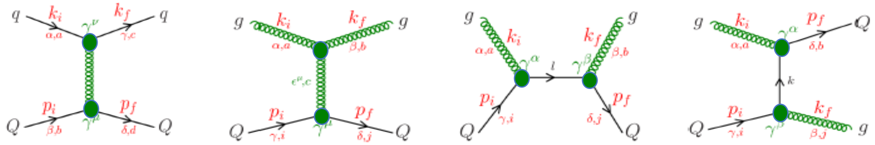

$$\mathcal{C}[f_Q] = \frac{1}{2E_1}\int\frac{d^3p_2}{2E_2(2\pi)^3}\int\frac{d^3p_1'}{2E_{1'}(2\pi)^3}$$
$$\times[f_Q(p_1')f_{q,g}(p_2') - f_Q(p_1)f_{q,g}(p_2)]$$
$$\times|\mathcal{M}_{(q,g)+Q}(p_1p_2\to p_1'p_2')|^2$$
$$\times(2\pi)^4\delta^4(p_1+p_2-p_1'-p_2')\ ,$$

M scattering matrix by QPM model fit to lQCD EoS

More details in:

M. L. Sambataro, et al., Phys. Lett. B **849**, 138480 (2024)
M. L. Sambataro, et al., Eur. Phys. J. C **82**, no.9, 833 (2022)
L. Oliva, S. Plumari and V. Greco, JHEP **05**, 034 (2021)
S. Plumari, et al., Phys. Lett. B **805**, 135460 (2020)
Y. Sun, S. Plumari and V. Greco, Eur. Phys. J. C **80**, no.1, 16 (2020)
S. Plumari, Eur. Phys. J. C 79, no.1, **2** (2019)
F. Scardina, et al., Phys. Rev. C **96**, no.4, 044905 (2017)

Quasi Particle Model (QPM)

Non perturbative dynamics → M scattering matrices (q,g → Q) evaluated by Quasi-Particle Model fit to **lQCD thermodynamics**

N_f=2+1
Bulk:
u,d,s

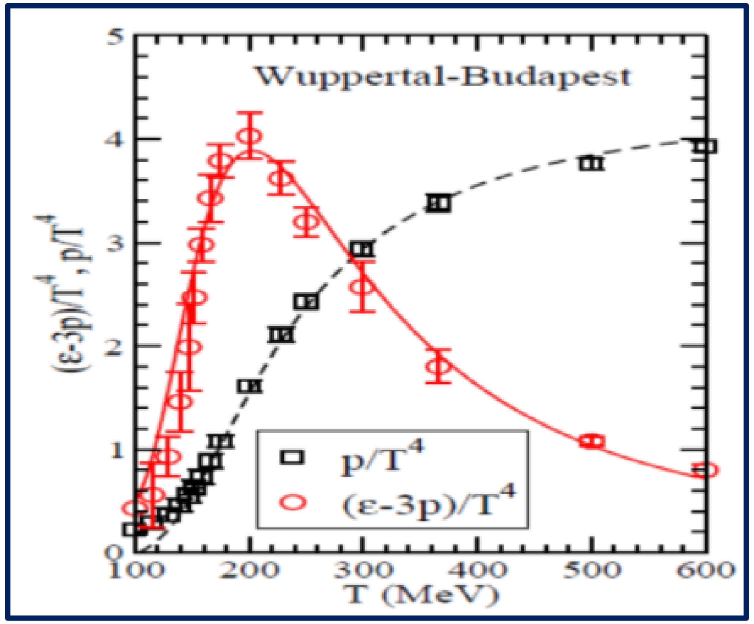

$$m_g^2(T) = \frac{2N_c}{N_c^2-1} g^2(T)\,T^2$$
$$m_q^2(T) = \frac{1}{N_c} g^2(T)\,T^2$$

→ **Thermal masses of gluons and light quarks**

g(T) from a fit to ε from lQCD data → good reproduction of P, ε-3P

$$g^2(T) = \frac{48\pi^2}{(11N_c - 2N_f)\ln\left[\lambda\left(\frac{T}{T_c} - \frac{T_s}{T_c}\right)\right]^2}$$

λ=2.6
T_s=0.57 T_c

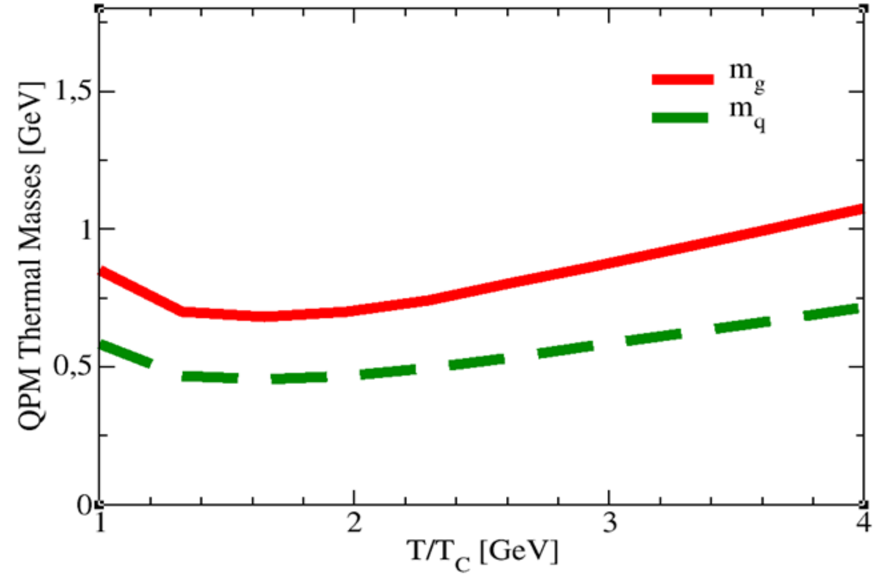

Larger than pQCD especially as T → T_c

S. Plumari et al, *Phys.Rev.D* 84 (2011) 094004
H. Berrehrah,, PHYSICAL REVIEW C **93**, 044914 (2016)

Indipendent fragmentation

Spectrum of heavy quarks produced in pp-collisions can be computed up to NLO in s with available tools

Transition from quark momentum spectrum to hadron momentum, using fragmentation model:

$$\frac{dN_h}{d^2p_h} = \sum_f \int dz \frac{dN_f}{d^2p_f} D_{f\to h}(z)$$

q → π, K, p, Λ ..

c → D, D_s, Λ_c, ...

Fragmentation function

- **Fragmentation functions** $D_{f\to h}$ are phenomenological functions to parameterize the *non-perturbative parton-to-hadron transition* (z = fraction of the parton momentum taken by the hadron h)

- **Fragmentation functions** assumed **universal** among energy and collision systems and constrained from e^+e^- and ep

- Different models for FFs are currently in use in literature:
  - Peterson et al., $D(z) = \frac{C}{z\left(1-\frac{1}{z}-\frac{\epsilon}{1-z}\right)^2}$
  - Kartvelishvili et al., $D(z) = C z^{\alpha}(1-z)$

Coalescence approach in phase space for HQ

For details see talk: V. Minissale [20 july 2024]

Statistical factor colour-spin-isospin

Parton Distribution function

Hadron Wigner function

$$\frac{dN_{Hadron}}{d^2p_T} = g_H \int \prod_{i=1}^{n} p_i \cdot d\sigma_i \frac{d^3p_i}{(2\pi)^3} f_q(x_i,p_i) f_W(x_1,\ldots,x_n;p_1,\ldots,p_n)\,\delta\left(p_T - \sum_i p_{iT}\right)$$

Wigner function <-> Wave function

$$\Phi_M^W(\mathbf{r},\mathbf{q}) = \int d^3r' e^{-i\mathbf{q}\cdot\mathbf{r}'} \varphi_M\left(\mathbf{r}+\frac{\mathbf{r}'}{2}\right)\varphi_M^*\left(\mathbf{r}-\frac{\mathbf{r}'}{2}\right)$$

$\varphi_M(\boldsymbol{r})$ *meson wave function*

Assuming gaussian wave function

$$f_M(x_1,x_2;p_1,p_2) = A_W \exp\left(-\frac{x_{r1}^2}{\sigma_r^2} - p_{r1}^2\sigma_r^2\right)$$

For baryon N_q=3

$$f_H(\ldots) = \prod_{i=1}^{N_q-1} A_W \exp\left(-\frac{x_{ri}^2}{\sigma_{ri}^2} - p_{ri}^2\sigma_{ri}^2\right)$$

For details of the model see:

S. Plumari, et al. Eur. Phys. J. C 78, no.4, 348 (2018)
V. Minissale, et al., Phys. Lett. B 821, 136622 (2021)
V. Minissale et al, arXiv:2405.19244 [hep-ph]
V. Minissale, et al., Eur. Phys. J. C 84, no.3, 228 (2024)

Wigner function **width** fixed by root-mean-square charge radius from **quark model**

C.-W. Hwang, EPJ C23, 585 (2002);
C. Albertus et al., NPA 740, 333 (2004)

$$\langle r^2\rangle_{ch} = \frac{3}{2}\frac{m_2^2Q_1 + m_1^2Q_2}{(m_1+m_2)^2}\sigma_{r1}^2 + \frac{3}{2}\frac{m_3^2(Q_1+Q_2)+(m_1+m_2)^2Q_3}{(m_1+m_2+m_3)^2}\sigma_{r2}^2 \qquad (8)$$

$\sigma_{ri} = 1/\sqrt{\mu_i\omega}$ Harmonic oscillator relation

$$\mu_1 = \frac{m_1m_2}{m_1+m_2}, \quad \mu_2 = \frac{(m_1+m_2)m_3}{m_1+m_2+m_3}.$$

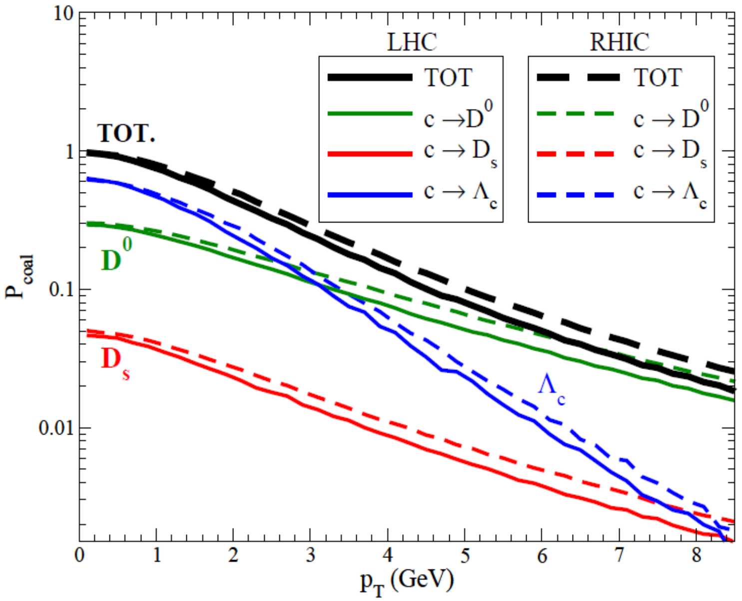

Normalization in $f_W(\ldots)$ *fixed by requiring*

$P_{coal}(p\to0)=1$:

charm not "coalescencing" undergo fragmentation:

$$\frac{dN_{had}}{d^2p_T\,dy} = \sum \int dz \frac{dN_{fragm}}{d^2p_T\,dy}\frac{D_{had/c}(z,Q^2)}{z^2}$$

charm number conserved at each p_T ,

we have employed e^+e^- FF now PYTHIA

Catania QPM: some predictions for charm

$$\epsilon_n = \frac{\langle r_\perp^n \cos[n(\varphi - \Phi_n)]\rangle}{\langle r_\perp^n \rangle} \qquad \Phi_n = \frac{1}{n}\arctan\frac{\langle r_\perp^n \sin(n\varphi)\rangle}{\langle r_\perp^n \cos(n\varphi)\rangle}$$

$$E\frac{d^3N}{dp_T} = \frac{1}{2\pi}\frac{d^2N}{p_T dp_T dy}\left\{1 + \sum_{i=1}^{\infty} v_n \cos[n(\varphi - \Psi_n)]\right\}$$

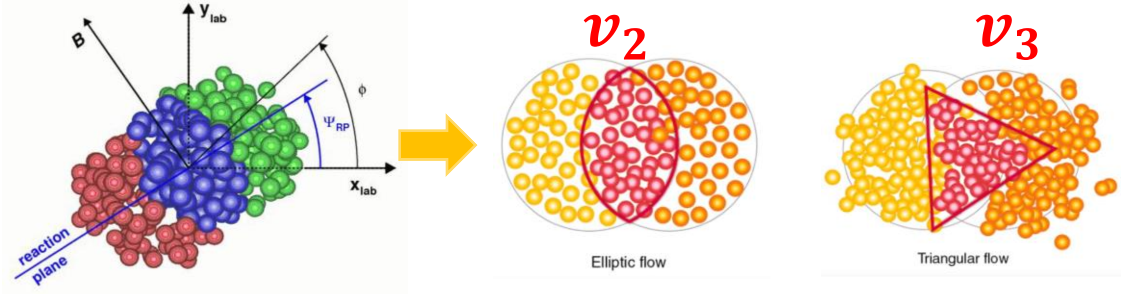

In 30-50 % centrality class → larger v_2 and comparable v_3

- ➢ v_2 mainly generated by the geometry of overlapping region
- ➢ v_3 mainly driven by the fluctuation of the initial triangularity

Data from ALICE coll.: *PLB* 813 (2021) 136054

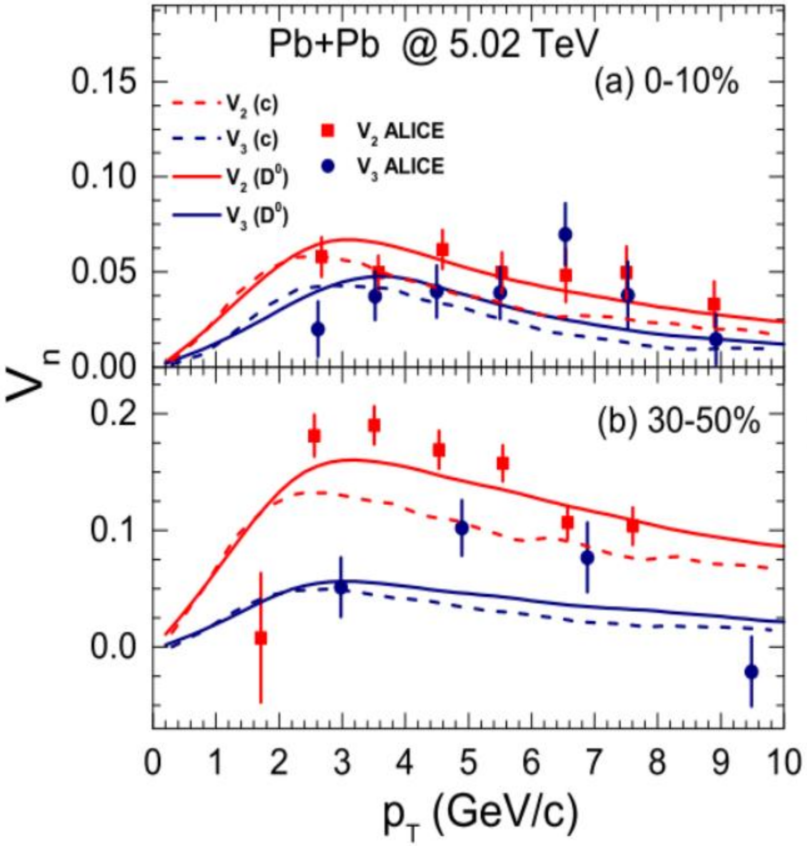

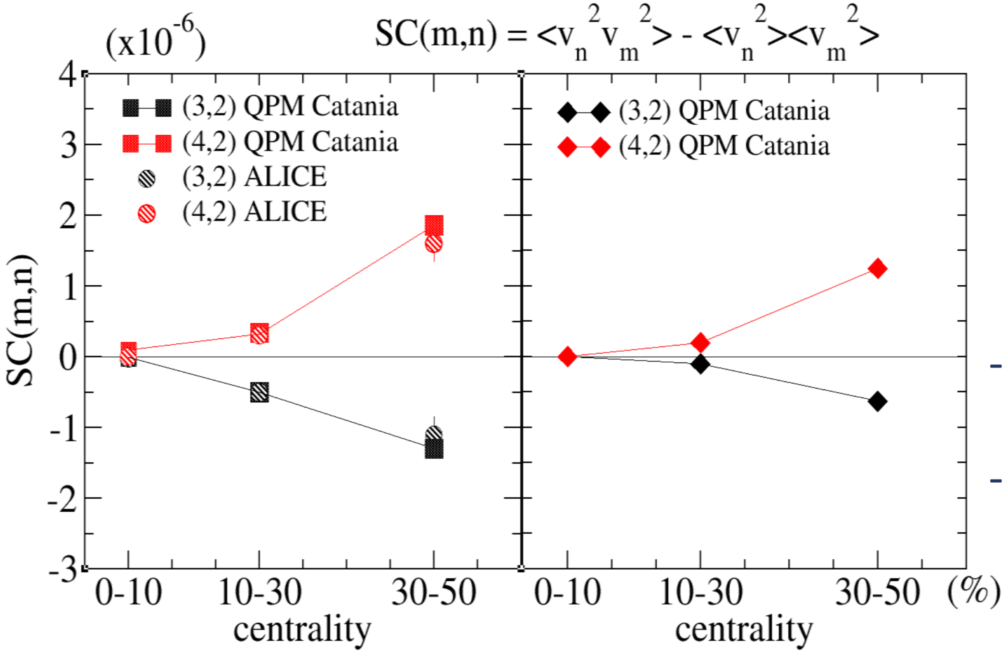

Data from: S. Mohapatra *NPA* 956 (2016) 59-66

Correlations between ε_n and ε_m
→ correlation v_n and v_m

- Good description of v_n- v_m corr. for bulk
- Prediction for weaker correlation between soft and hard particles

M. L. Sambataro et al., EPJ C 82, no.9, 833 (2022)

S. Plumari et al., PLB 805, 135460 (2020)

Extension to bottom dynamics: R_{AA}

No parameters changed
with respect to charm dynamics → same interaction

Data from: ALICE coll., arxiv:2211.13985

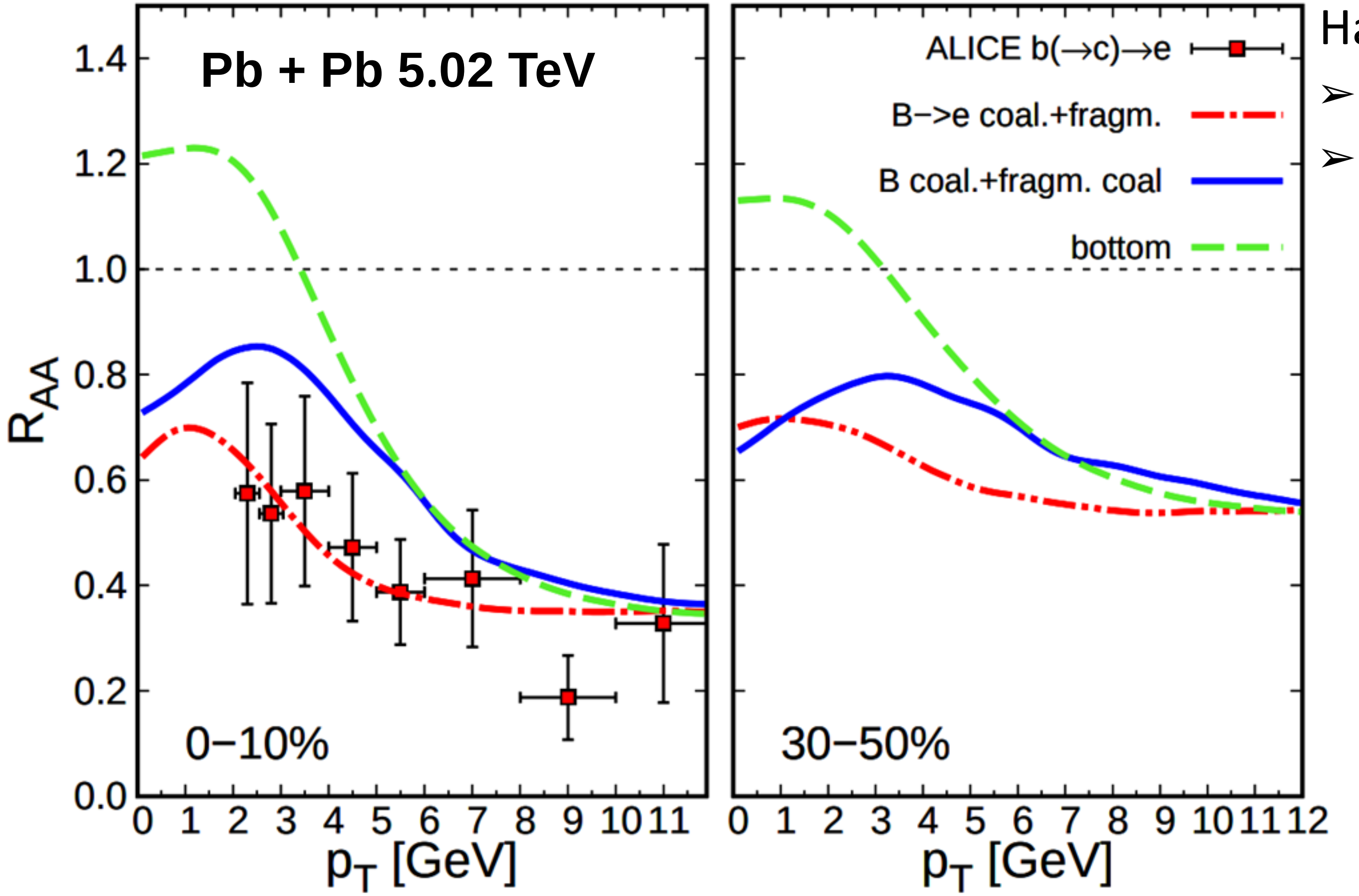

Hadronization with coalescence + fragmentation model

- ➢ Prediction for B meson R_{AA}
- ➢ R_{AA} of electrons from semileptonic B meson decay

- Shift of the peak to higher momenta
  → smaller with respect to the one for D mesons in the same model.

M.L. Sambataro et al., *Phys.Lett.B* 849 (2024) 138480

Extension to bottom dynamics: $v_2(p_T)$, $v_3(p_T)$

No parameters changed with respect to charm dynamics → same interaction

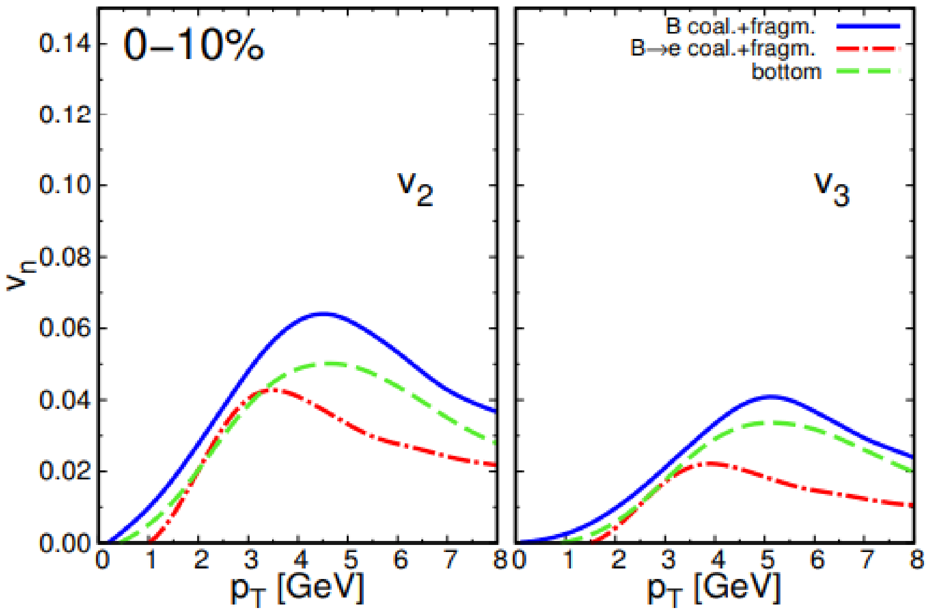

Data from ALICE, PRL 126, 162001 (2021)

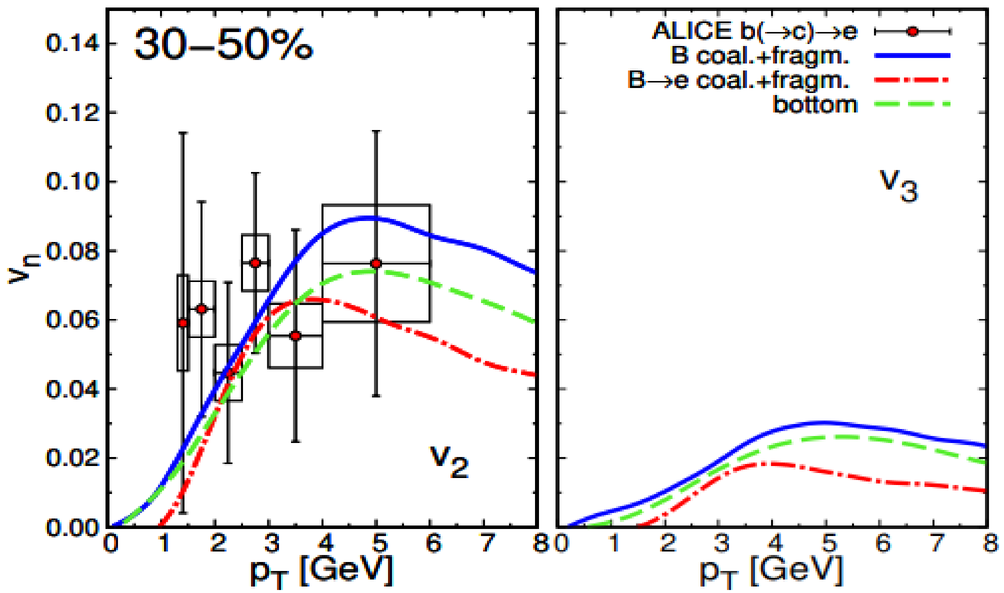

Compared to charm quark:

- Efficiency of conversion of ε_2 :
  15% smaller for v_2 in most central collisions.
  40% smaller for v_2 at 30–50% centrality.

- Efficiency of conversion of ε_3 :
  30% smaller for v_3 at both 0-10% and 30-50% centralities.

From central to peripheral:

- enhancement of v_2 (ε_2(0-10%)≃0.13 and ε_2(30-50%)≃0.42)
- similar v_3 (ε_3(0-10%)≃0.11 and ε_3(30-50%))≃0.21)

M.L. Sambataro et al., *Phys.Lett.B* 849 (2024) 138480

MOMENTUM DEPENDENT Quasi Particle Model:

QPM vs QPMp

Going back to Quasi Particle Model (QPM)…

Equation of State and Susceptibilities

Non perturbative dynamics → M scattering matrices (q,g → Q) evaluated by Quasi-Particle Model fit to **lQCD thermodynamics**

N_f=2+1
Bulk:
u,d,s

QPM Standard

no momentum dependence

$$m_g^2(T) = \frac{2N_c}{N_c^2-1} g^2(T)\, T^2$$
$$m_q^2(T) = \frac{1}{N_c} g^2(T)\, T^2$$

→ **Thermal masses of gluons and light quarks**

g(T) from a fit to ε from lQCD data → good reproduction of P, ε-3P

Standard QPM understimates the **quark susceptibilities**

$$g^2(T) = \frac{48\pi^2}{(11N_c - 2N_f)\ln\left[\lambda\left(\frac{T}{T_c} - \frac{T_s}{T_c}\right)\right]^2}$$

λ=2.6
T_s=0.57 T_c

Larger than pQCD especially as T → T_c

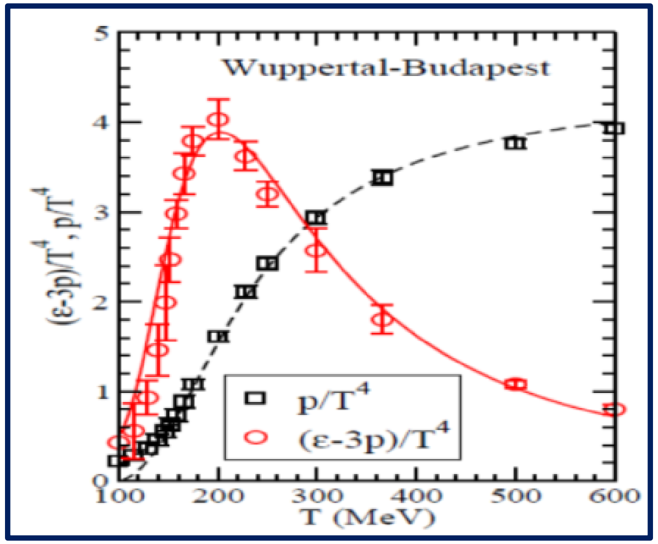

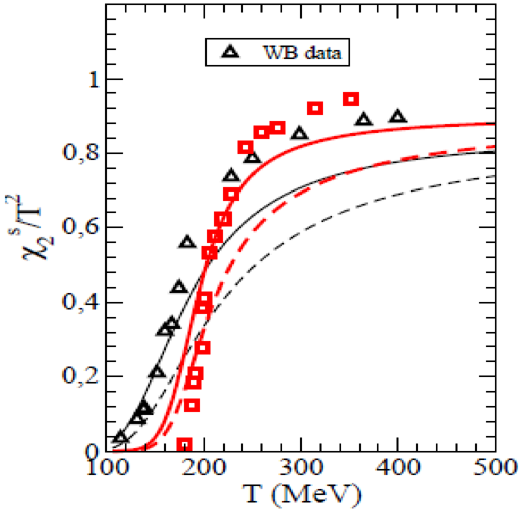

S. Plumari et al, *Phys.Rev.D* 84 (2011) 094004
H. Berrehrah,, *Phys.Rev.* C **93**, 044914 (2016)

QPM extension: QPMp(N_f=2+1+1)

Dyson-Schwinger studies in the vacuum → following the model developed by PHSD group

H. Berrehrah, W. et al., Phys.Rev.C 93, 044914 (2016).
C. S. Fischer, J. Phys. G 32, R253 (2006).
M.L. Sambataro et al. e-Print: 2404.17459

$$M_g(T,\mu_q,p) = \left(\frac{3}{2}\right)\left(\frac{g^2(T^\star/T_c(\mu_q))}{6}\left[\left(N_c+\frac{1}{2}N_f\right)T^2+\frac{N_c}{2}\sum_q\frac{\mu_q^2}{\pi^2}\right]\left[\frac{1}{1+\Lambda_g(T_c(\mu_q)/T^\star)p^2}\right]\right)^{1/2}+m_{\chi g}$$

$$M_{q,\bar{q}}(T,\mu_q,p) = \left(\frac{N_c^2-1}{8N_c}g^2(T^\star/T_c(\mu_q))\left[T^2+\frac{\mu_q^2}{\pi^2}\right]\left[\frac{1}{1+\Lambda_q(T_c(\mu_q)/T^\star)p^2}\right]\right)^{1/2}+m_{\chi q}$$

Momentum dependent factors

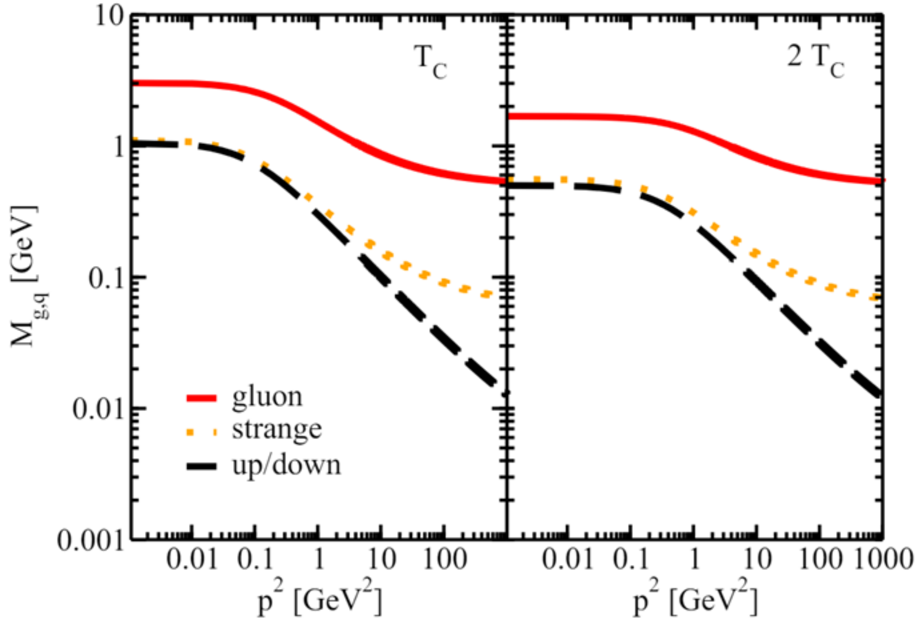

We correctly reproduce both **EoS** and **quark susceptibilities** which are understimated in the standard QPM approach.

Pressure, trace anomaly **including charm** Nf=2+1+1

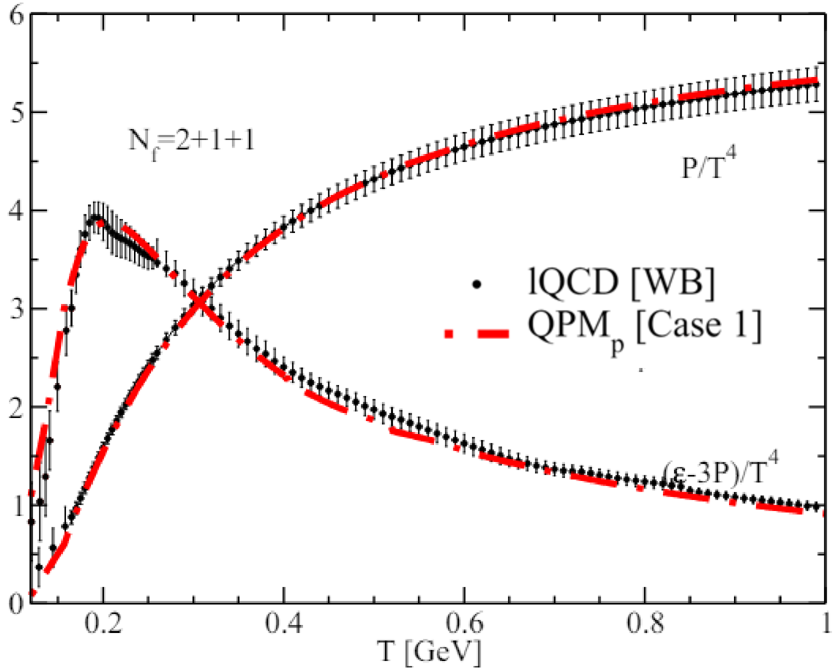

QPM extension: QPMp(N_f=2+1+1) and m_c (T)

we have also extended our quasi-particle model approach for **Nf = 2+1** to **Nf = 2 + 1 + 1** where the **charm quark is included**

Temperature parametrization for charm mass:

Case 1: $m_c = 1.5\ GeV$

Case 2: $m_c^2 = m_{c0}^2 + \frac{N_c^2-1}{8N_c} g^2 [T^2 + \frac{\mu_c^2}{\pi^2}]$ with $m_{c0} = 1.3\ GeV$

Case 3: m_c fixed by charm fluctuation $\chi_2^c = \frac{T}{V}\frac{\partial^2 \ln Z}{\partial \mu_i^2}$

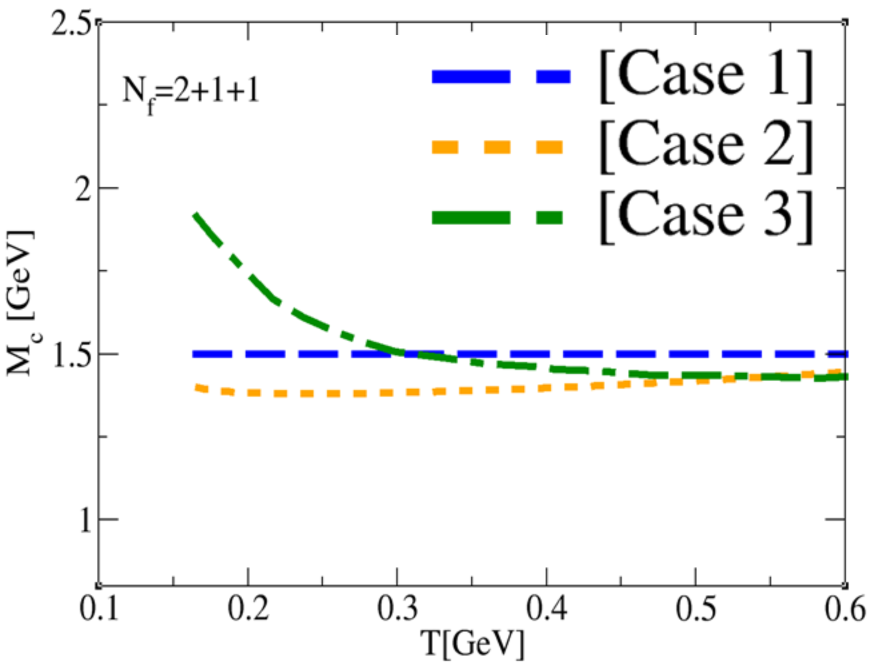

M.L. Sambataro et al. e-Print: 2404.17459

QUARK SUSCEPTIBILITIES

$$\chi_{u,s,c} = \frac{T}{V}\frac{\partial^2 \ln Z}{\partial \mu_{u,s,c}^2}$$

STRANGE

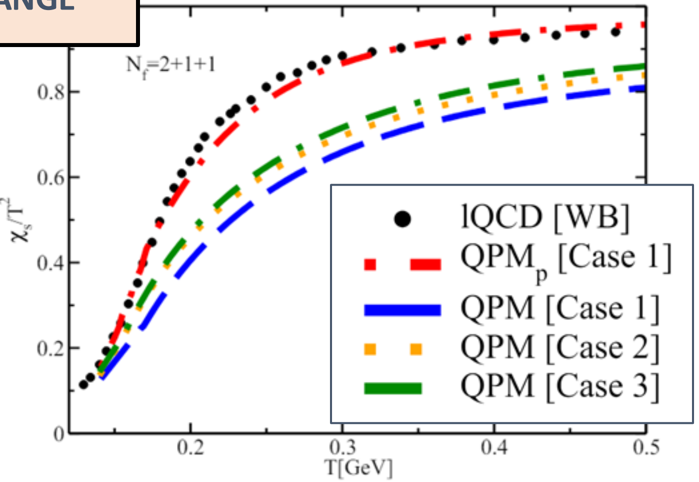

LIGHT

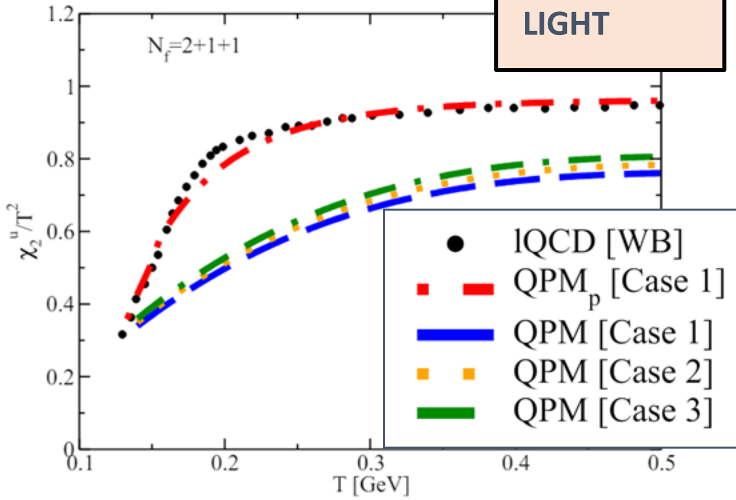

QPM understimates the lQCD data;
QPMp -> smaller 'thermal average mass' -> extra contribution in susceptibility

QPM extension: QPMp(N_f=2+1+1) and m_c (T)

we have also extended our quasi-particle model approach for **Nf = 2+1** to **Nf = 2 + 1 + 1** where the **charm quark is included**

Temperature parametrization for charm mass

Case 1: $m_c = 1.5\ GeV$

Case 2: $m_c^2 = m_{c0}^2 + \frac{N_c^2-1}{8N_c} g^2 [T^2 + \frac{\mu_c^2}{\pi^2}]$ with $m_{c0} = 1.3\ GeV$

Case 3: m_c fixed by charm fluctuation $\chi_2^c = \frac{T}{V} \frac{\partial^2 \ln Z}{\partial \mu_i^2}$

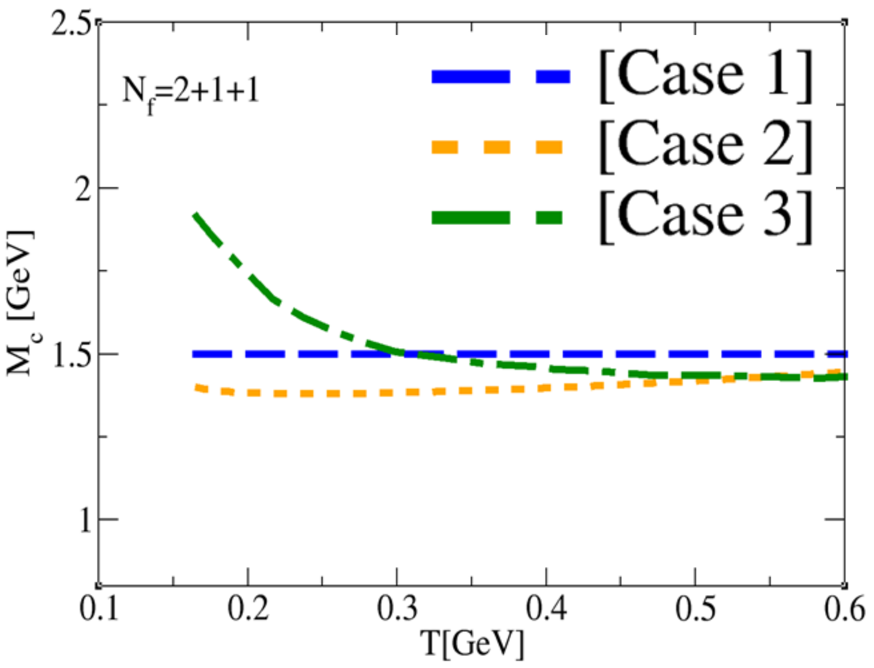

M.L. Sambataro et al. e-Print: 2404.17459

QUARK SUSCEPTIBILITIES

$$\chi_{u,s,c} = \frac{T}{V} \frac{\partial^2 \ln Z}{\partial \mu_{u,s,c}^2}$$

CHARM

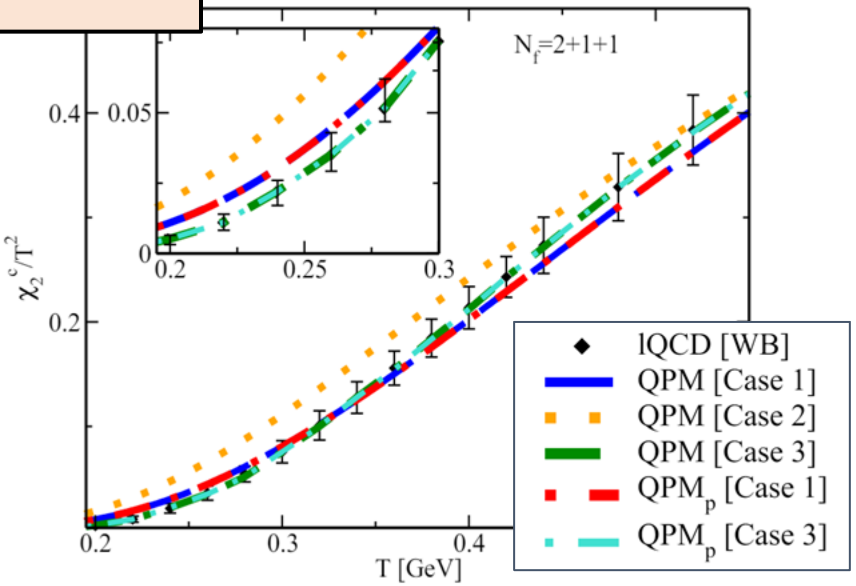

- lQCD data overestimated for T≈0.2-0.3 GeV with constant m_C.

- **Disfavored**: increasing m_C(T) and m_C smaller than 1.5 GeV

- Susceptibility implies a decreasing m_C(T) from 1.9 at T_C down to 1.5 at $2T_C$.

QPMp – spatial diffusion coefficient D_S

Spatial diffusion coefficient D_s → standard QPM
standard QPM including charm
extended QPM

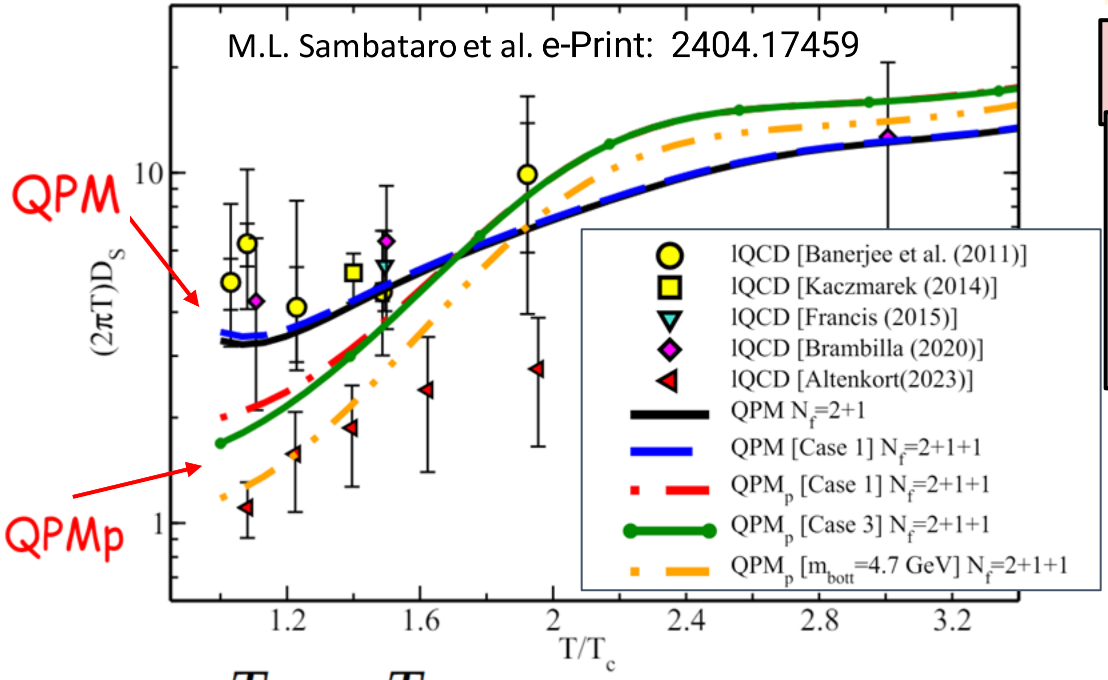

$$D_s = \frac{T}{M\,\gamma} = \frac{T}{M}\,\tau_{th}$$

QPMp

T/T_c <1.6 -> strong non-perturbative behaviour of D_S.

high T region -> D_S grows toward the pQCD estimate faster than QPM

QPMp for charm Case 3 and bottom (M=4.7 GeV): closer to D_S lQCD which include dynamical fermions

in the p → 0 limit

From D_s we obtain at T_c :

- **τ_{th}(c , p=0) ~ 6 fm/c (QPM) -> 4 fm/c (QPMp)**
- **τ_{th}(b , p=0) ~ 13 fm/c (QPM) -> 7 fm/c (QPMp)**

QPMp – spatial diffusion coefficient D_S

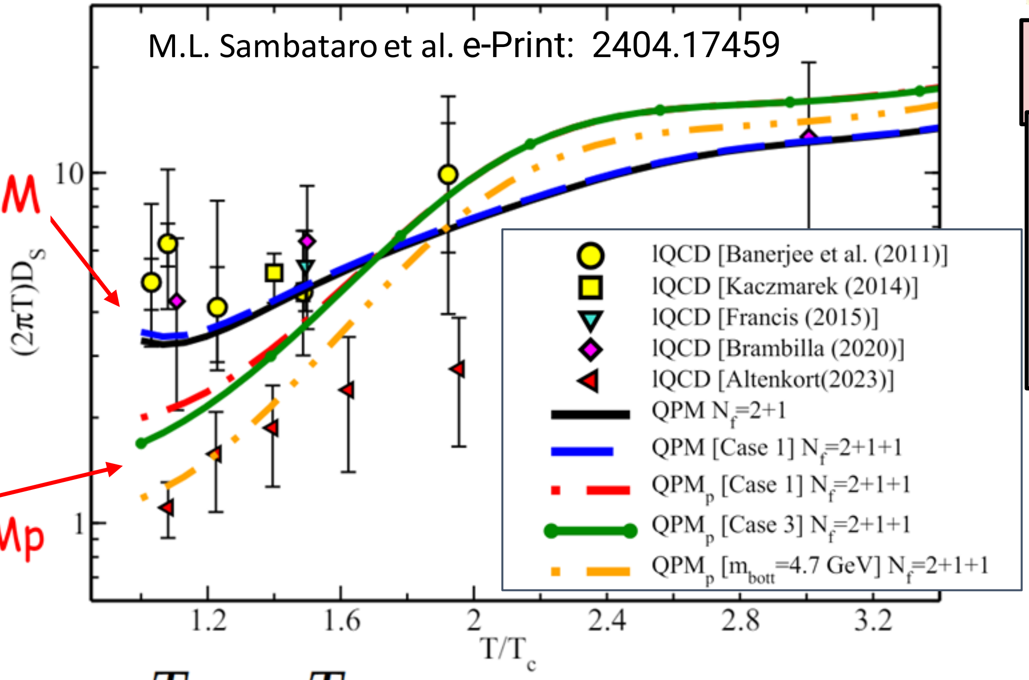

$$D_s = \frac{T}{M\,\gamma} = \frac{T}{M}\,\tau_{th}$$

Spatial diffusion coefficient D_s → standard QPM
standard QPM including charm
extended QPM

QPMp

T/T_c <1.6 -> strong non-perturbative behaviour of D_S.

high T region -> D_S grows toward the pQCD estimate faster than QPM

QPMp for charm Case 3 and bottom (M=4.7 GeV): closer to D_S lQCD which include dynamical fermions

τ_{th} for charm

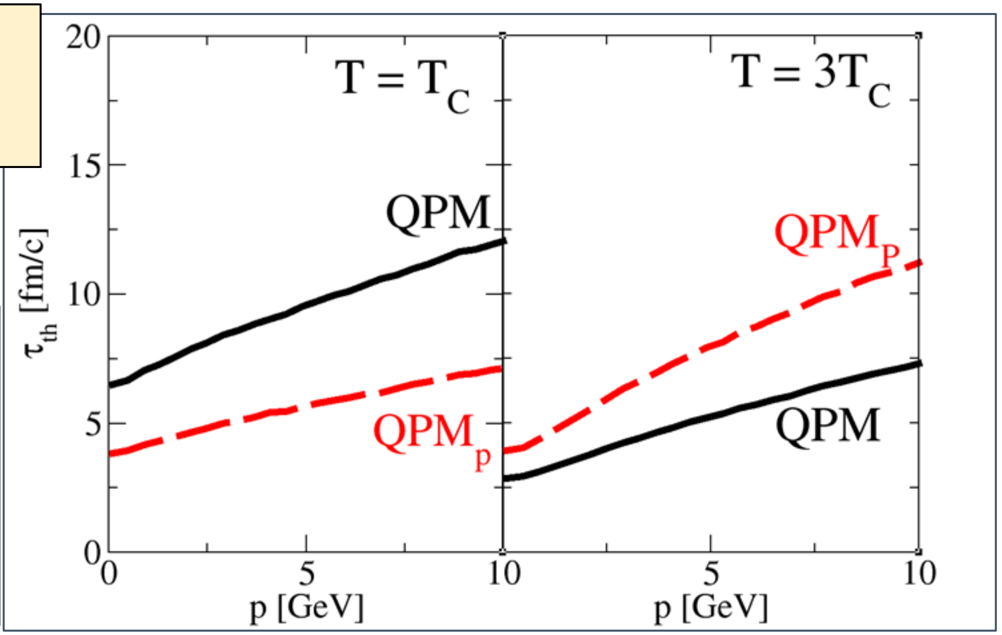

T=T_C -> 40 % larger τ_{th} for both QPM and QPMp at at finite momentum (~5 GeV)

T=3T_C QPMp -> more perturbative dynamics -> larger τ_{th} wrt QPM
finite momentum (~5 GeV) -> 50 % larger τ_{th}

QPMp – spatial diffusion coefficient D_S

Spatial diffusion coefficient D_s → standard QPM

standard QPM including charm

extended QPM

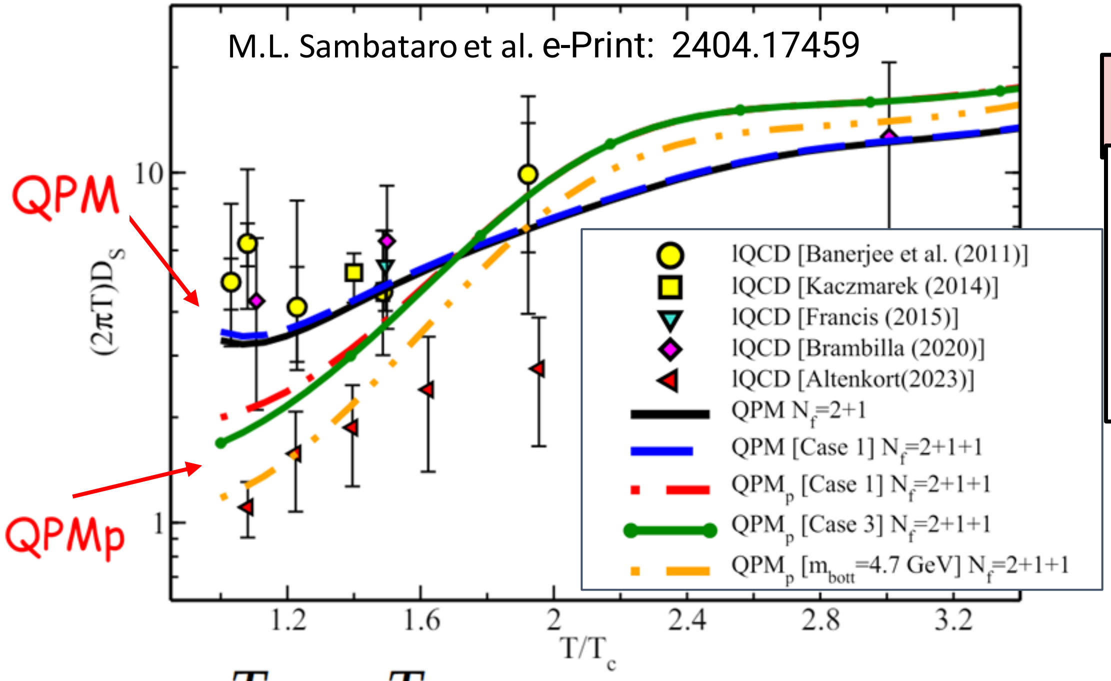

$$D_s = \frac{T}{M\,\gamma} = \frac{T}{M}\,\tau_{th}$$

QPMp

T/T_c <1.6 -> strong non-perturbative behaviour of D_S.

high T region -> D_S grows toward the pQCD estimate faster than QPM

QPMp for charm Case 3 and bottom (M=4.7 GeV): closer to D_S lQCD which include dynamical fermions

$M^* = 20 M_c$ -> saturated D_S (M)

standard QPM

extended QPM

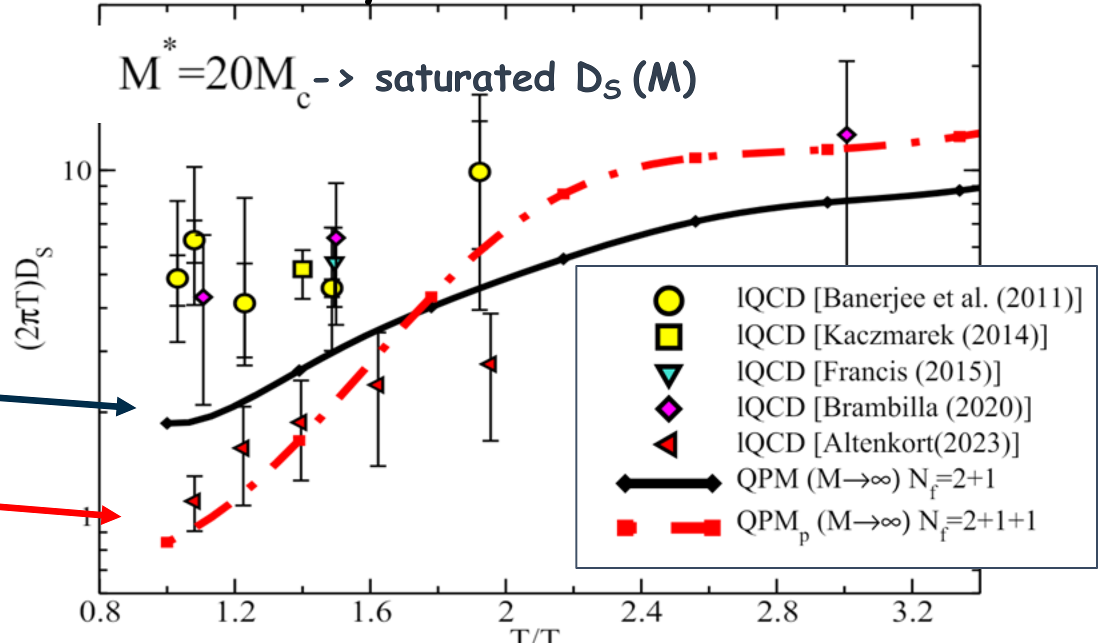

QPM vs QPMp in the infinite mass limit?

bottom (M=4.7 GeV): very close to infinite mass limit

QPMp – spatial diffusion coefficient D_S

Spatial diffusion coefficient D_s → standard QPM
standard QPM including charm
extended QPM

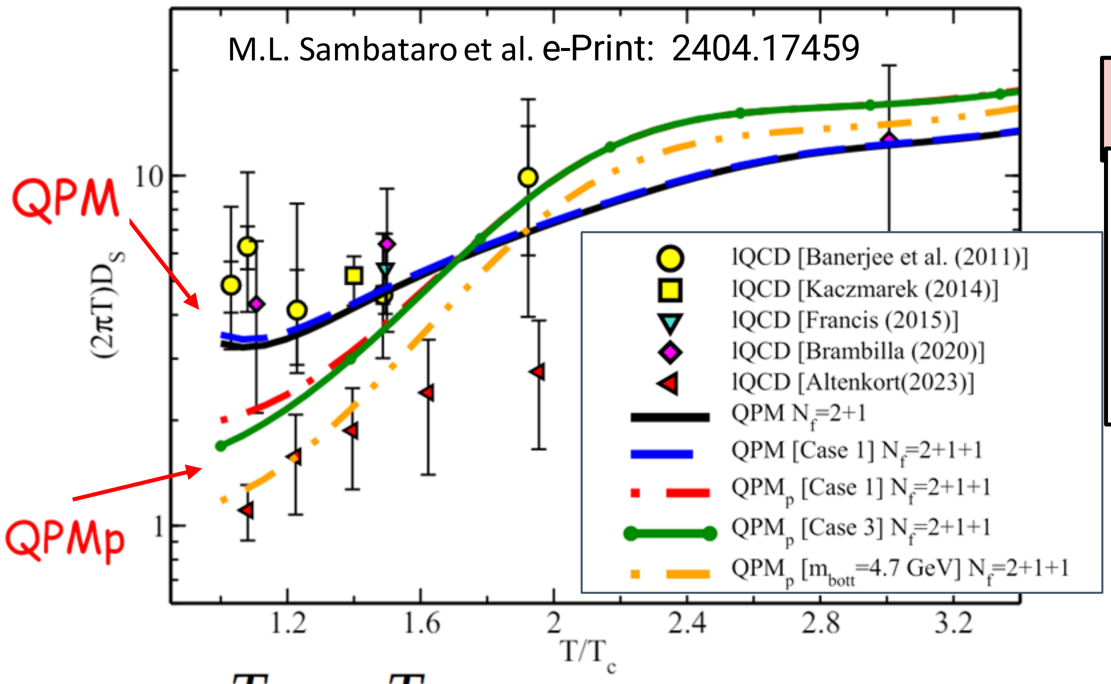

$$D_s = \frac{T}{M\,\gamma} = \frac{T}{M}\,\tau_{th}$$

QPMp

T/T_c <1.6 -> strong non-perturbative behaviour of D_S.

high T region -> D_S grows toward the pQCD estimate faster than QPM

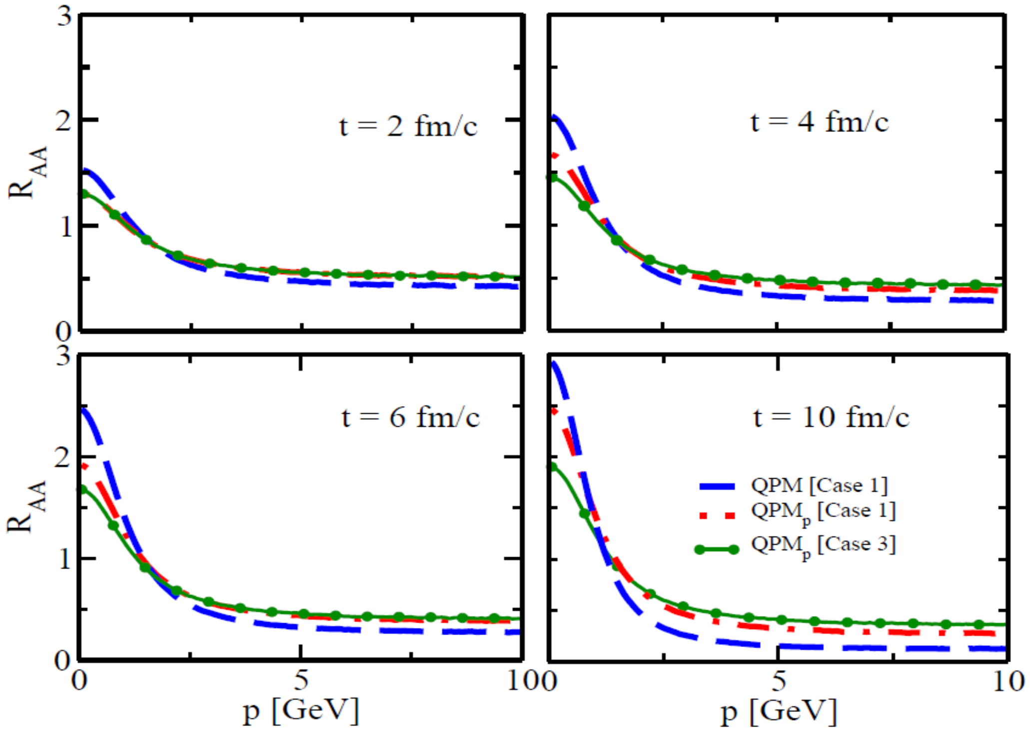

Conclusions

- **Extension to bottom quark dynamics in standard QPM**: good description of R_{AA} and v_2 of electrons from semileptonic B meson decay and prediction for v_2 and v_3

- **Charm mass [T] parametrization:** charm susceptibility as function of T implies a decreasing m_C(T) from 1.9 at T_C down to 1.5 at $2T_C$ getting closer to lQCD data for Ds.

- **QPMp**
  Good reproduction of both EoS and susceptibilities -> decrease of D_s at small T.
  Bottom D_s very close to the new lQCD data for M->∞.
- **Spatial diffusion coefficient D_s(T) in the infinite mass limit ->** satisfactory agreement with the lQCD calculations that include dynamical fermions, differently from previous lQCD data in quenched approximation.

  - Perspectives: Effect on observables for realistic simulations.

Catania QPM: some prediction for charm…

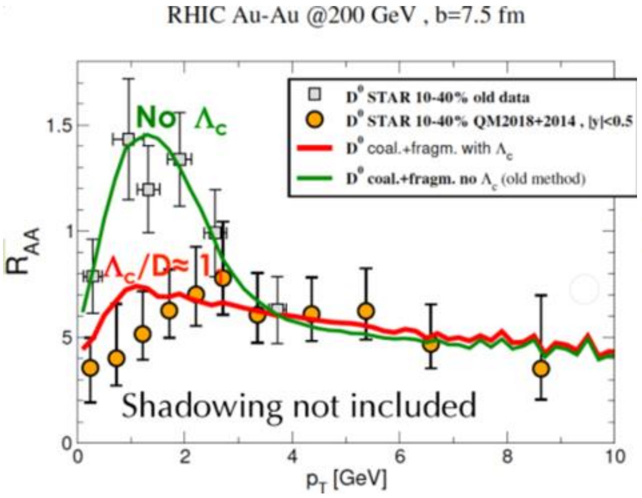

Scardina et al., PRC 97(2017)

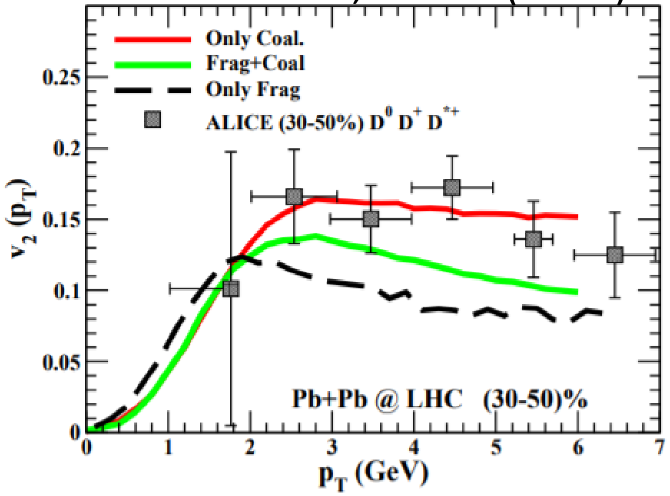

Good description of

R_{AA}, v_2 at RHIC & LHC energies within error bars

Monte Carlo Glauber for initial condition of partons

S.Plumari et al, *Phys.Rev.C* 92 (2015) 5

Predictions for D mesons

- **Event-Shape Engeenering Technique:**
  Prediction for similar correlation for hard particles wrt bulk

v_n - v_m correlations

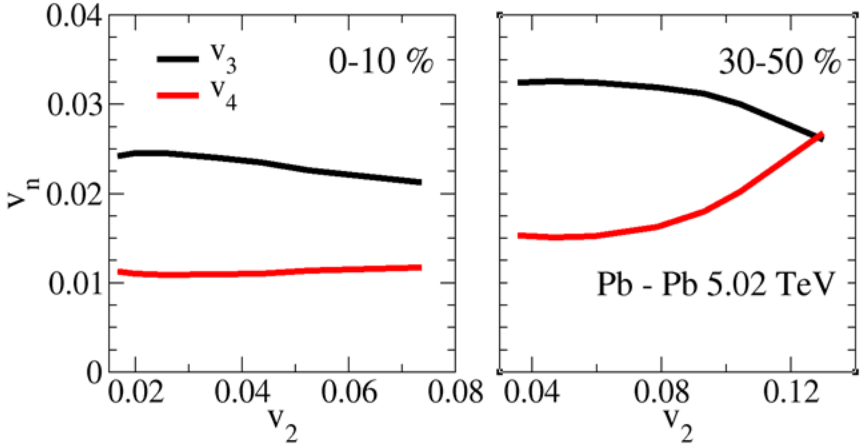

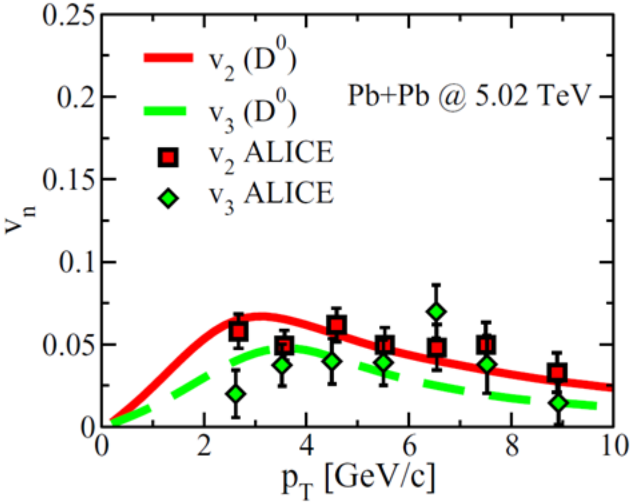

Triangular flow v_3

ALICE collaboration, *Phy*

M.L. Sambataro, et al., *Eur.Phys.J.C* 82 (2022)

LHC: results

Data from ALICE Coll. JHEP 1209 (2012) 112

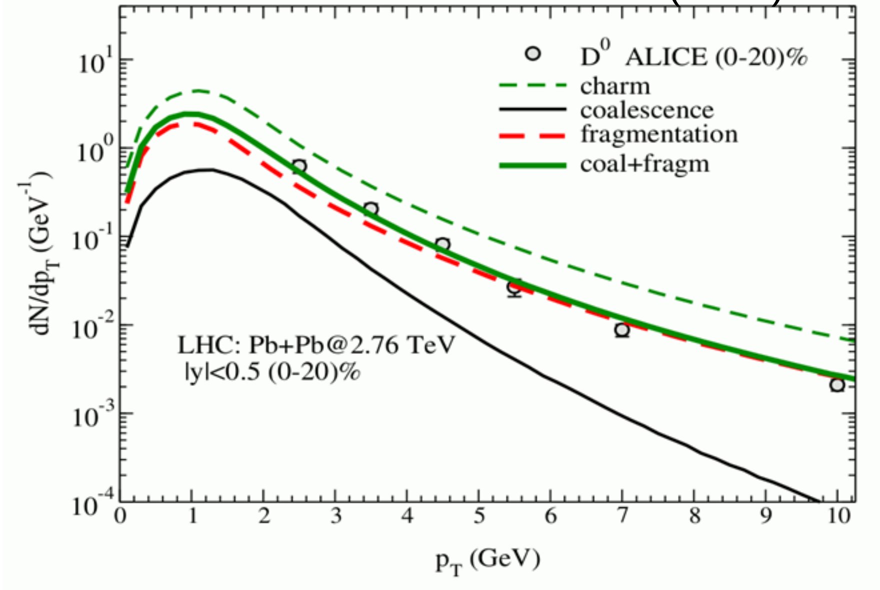

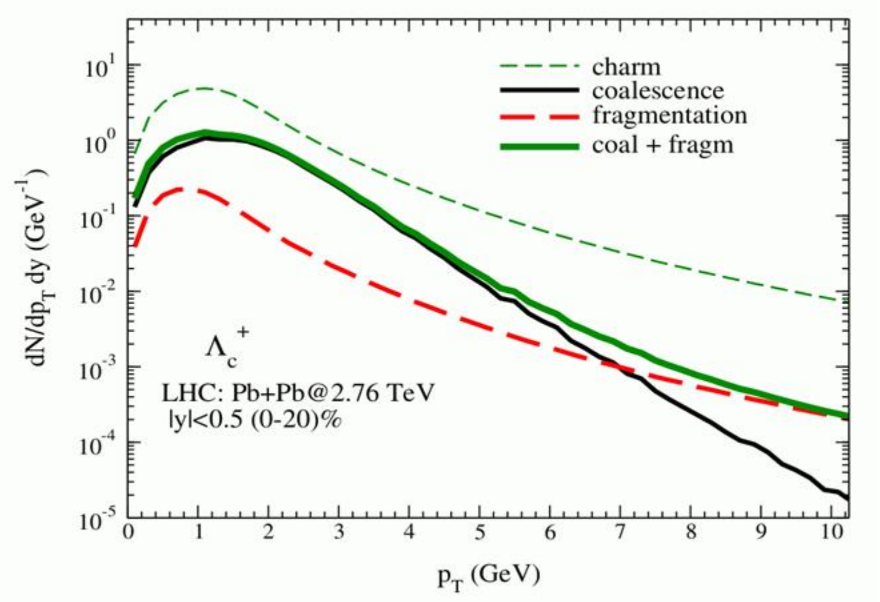

wave function widths σ_p of baryon and mesons kept the same at RHIC and LHC!

STAR coll. arXiv:1910.14628

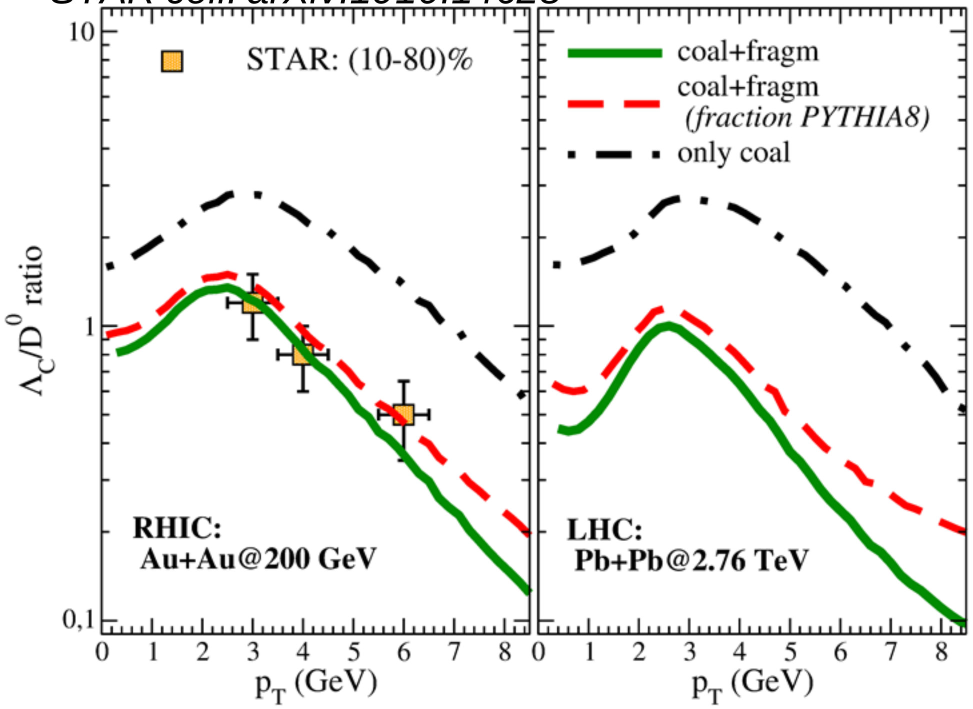

The Λ_c/D^0 ratio is smaller at LHC energies: fragmentation play a role at intermediate p_T

S. Plumari, et al., Eur. Phys. J. ***C78*** *no. 4, (2018) 348*

LHC: results

Results for 0-10% in PbPb @5.02TeV:

Consistent with the trend shown at RHIC and LHC @2.76TeV

Available data at low p_T → differences recombination vs SHM

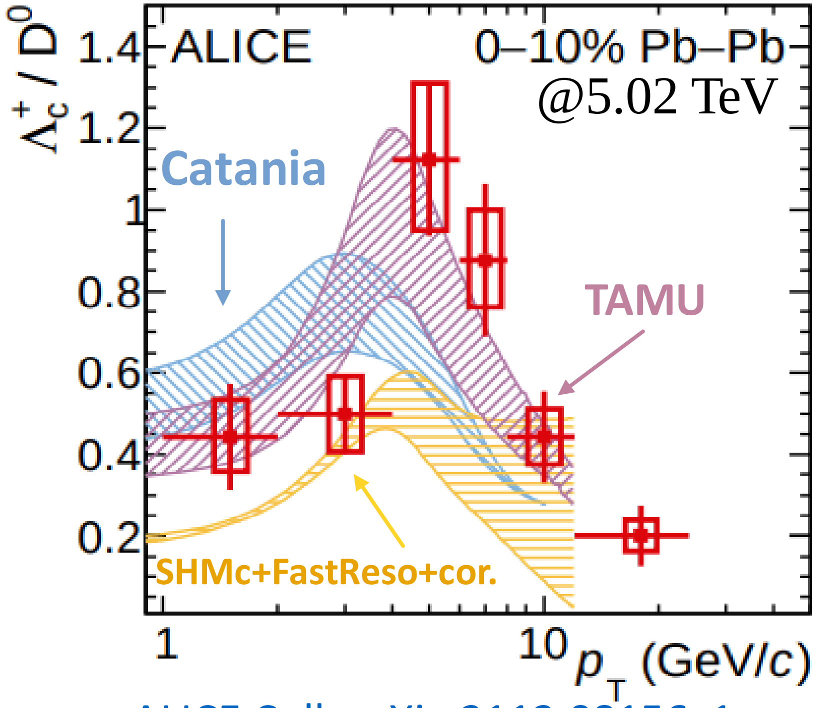

ALICE Coll. arXiv:2112.08156v1

wave function widths σ_p of baryon and mesons kept the same at RHIC and LHC!

STAR coll. arXiv:1910.14628

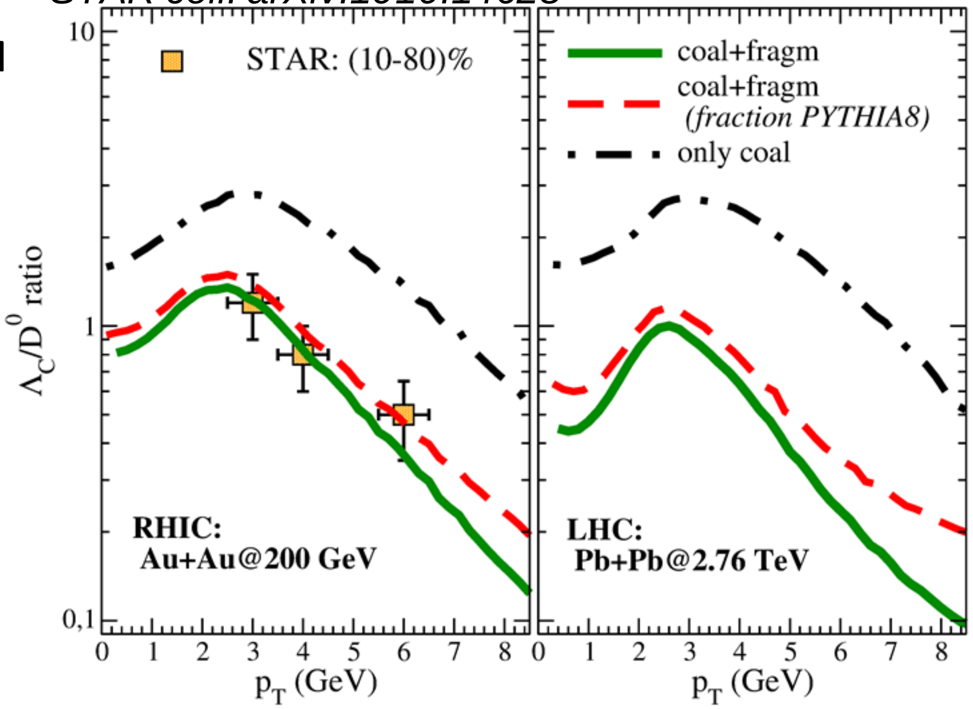

The Λ_c/D^0 ratio is smaller at LHC energies: fragmentation play a role at intermediate p_T

S. Plumari, et al., Eur. Phys. J. ***C78*** *no. 4, (2018) 348*